Organic Geochemistry 68 (2014) 107–117

Contents lists available at ScienceDirect

Organic Geochemistry

journal homepage: www.elsevier.com/locate/orggeochem

The origin of solid bitumen in the Honghuayuan Formation (O_1h) of the Majiang paleo-reservoir—Evidence from catalytic hydropyrolysates

Yunxin Fang [a,b], Yuhong Liao [a,*], Liangliang Wu [a], Ansong Geng [a]

[a] State Key Laboratory of Organic Geochemistry, Guangzhou Institute of Geochemistry, Chinese Academy of Sciences, Guangzhou 510640, China
[b] Guangzhou Marine Geological Survey, Guangzhou 510075, China

ARTICLE INFO

Article history:
Received 22 July 2013
Received in revised form 8 January 2014
Accepted 14 January 2014
Available online 25 January 2014

ABSTRACT

Large amounts of solid bitumen occur in the Honghuayuan Formation of the Lower Ordovician (O_1h) within the Majiang paleo-reservoir. Most of the potential source rocks and solid bitumens in the Southern Guizhou Depression are of high maturity (%Ro > 2). Consequently, the yields of extractable organic matter (EOM) from the potential source rocks and solid bitumens are too low to satisfy the requirement of instrumental analysis. Moreover, the reliability of oil–source correlations based on biomarkers in EOM may be questionable because the routine biomarkers obtained by Soxhlet extraction may have been severely altered by secondary alterations. In this research, catalytic hydropyrolysis (HyPy) is used to release covalently bound biomarkers from highly overmature kerogens and solid bitumens. We analyzed the covalently bound biomarkers and *n*-alkanes released from the O_1h solid bitumens and potential source rock kerogens via catalytic hydropyrolysis by using gas chromatography–mass spectrometry and gas chromatography–isotope ratio mass spectrometry to clarify the oil–source correlation of the Majiang paleo-reservoir. Compared with free biomarkers in EOM, the covalently bound biomarkers released by HyPy exhibit low-maturity characteristics and they retain inherited geochemical information. The oil–source correlation indicates that the Lower Cambrian marine mudstones are the main source for the O_1h solid bitumens of the Majiang paleo-reservoir. Furthermore, this research also suggests that some of the O_1h solid bitumens had suffered severe biodegradation ahead of thermal alteration.

1. Introduction

In the marine sequences of southern China, paleo-reservoirs occur extensively from Permian to Precambrian strata (Zhao et al., 2004; Liao et al., 2012). The Majiang paleo-reservoir, located in the Southern Guizhou Depression, is one of the biggest paleo-reservoirs formed during the Caledonian period in southern China. Only solid bitumens are left in the Majiang paleo-reservoir because the reservoir had been breached by continuous tectonic orogenies since the Caledonian. The solid bitumens of the Majiang paleo-reservoir are stored mainly in the pores and structural fissures of carbonates in the Lower Ordovician Honghuayuan Formation (O_1h) (Wu, 1989; Fang et al., 2011). Some of the solid bitumens in the Honghuayuan Formation are of high maturity (%Ro > 2%) owing to severe thermal maturation resulting from deep burial. Additionally, Xue et al. (2007) and Fang et al. (2011) pointed out that some O_1h paleo-reservoirs in the Majiang area had experienced severe evaporation, oxidation and biodegradation when the reservoirs were uplifted and the caprock was eroded. Previous studies (Ma et al., 2004; Chen et al., 2006; Tian et al., 2006; Ding et al., 2007; Tenger et al., 2008) have provided much information on the geological structure and oil–source correlation in the study area. There are three potential source rocks in this area: dark mudstone in the Lower Cambrian Niutitang Formation $\in_1n$, black shale in the Lower Silurian Longmaxi Formation (S_1l), and mudstone in the Lower Permian Qixia Formation (P_1q). The Lower Cambrian Niutitang Formation $\in_1n$ dark marine mudstones occurred widely in the Upper Yangtze region. In the study area, thick (~200–300 m) $\in_1n$ dark marine mudstones have high total organic carbon (TOC ~ 7%) of originally oil prone Type II kerogen at high maturities (reflectance > 1.8%). The Lower Cambrian mudstones entered an oil window between the Late Cambrian and the Early Ordovician (Fig. 1), reaching their oil generation peak between the Late Ordovician and the Early Devonian (Li et al., 2003). The reflectance (R_o) values of kerogen and bitumen in the Lower Cambrian mudstones exceed 2.5% currently. However, in the neighboring eastern Kaili area such as the Taijiang area, the source rocks have much lower maturities. The Lower Cambrian source rocks in the eastern Kaili area have subsided and been uplifted three times (Fig. 1). The ultimate R_o values of the Lower Cambrian source rocks reached ~1.4%.

* Corresponding author. Tel.: +86 20 85291567; fax: +86 20 85290706.
E-mail address: liaoyh@gig.ac.cn (Y. Liao).

http://dx.doi.org/10.1016/j.orggeochem.2014.01.008
0146-6380/

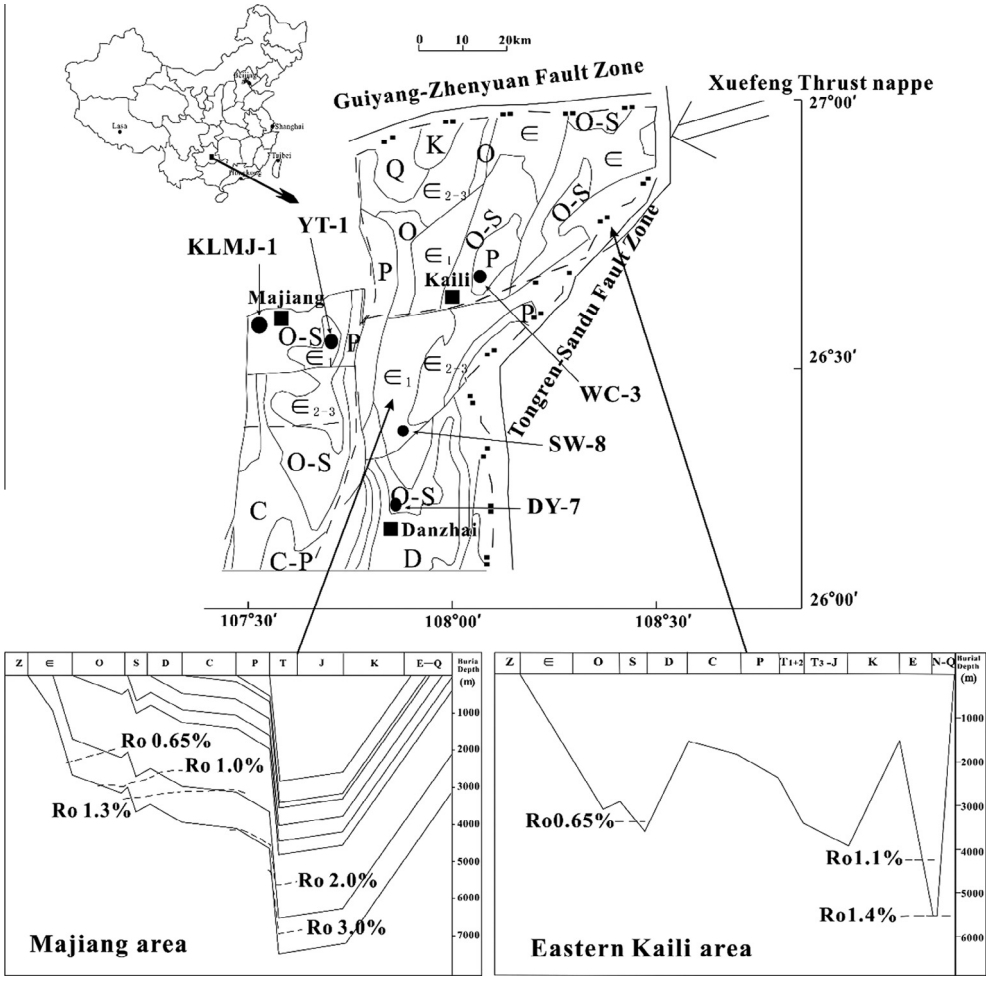

Fig. 1. Map showing sampling locations and the study area (modified from Xu et al., 2010), evolution thermal maturity of the source rocks in the Majiang area (Li et al., 2003) and the eastern Kaili area (Ma et al., 2004).

Several younger strata within the study area contain source rocks. The thick (110 m maximum) Lower Silurian Longmaxi Formation (S_1l) black shales under the Xuefeng thrust nappe and in the Upper Middle Yangtze contain high concentrations (TOC 5% max.) of Type IIa kerogen The Lower Permian Qixia Formation (P_1q) contains rocks with lower concentrations (TOC 2% max) of Type II kerogen at moderate maturity. Many Permian oil seepages and solid bitumens in the study area have been correlated to P_1q source rock (Zhang et al., 2007; Fang et al., 2011).

The source rocks of the O_1h solid bitumens in the study area are under debate because of multiphase tectonic movement and lack of reliable oil–source correlation based on biomarkers. In some of the previous literature (Wu, 1989; Tian et al., 2006; Hu et al., 2007; Zhang et al., 2007; Tenger et al., 2008; Fang et al., 2011), the O_1h solid bitumens in the Majiang paleo-reservoir were deemed to be mainly generated from the Lower Cambrian marine mudstones. Other researchers pointed out that the O_1h solid bitumens in the Majiang paleo-reservoir may be generated from both Lower Cambrian marine mudstones and Lower Silurian shales in the Xuefeng thrust nappe (Qiu et al., 1994), which is located to the east of the Majiang paleo-reservoir. Some even held the point of view that the Lower Permian mudstone in the eastern Kaili area could be a potential source rock of O_1h solid bitumens (Qiu et al., 1994; Ma et al., 2004). Given the multiple phase tectonic movement, stratigraphic overturning, unconformities, and extensive faults in this area, the possibility of Permian mudstone being the source rocks of O_1h bitumen cannot be excluded.

Most of the O_1h solid bitumens in the Majiang paleo-reservoir and Paleozoic source rocks, except for the Lower Permian source rocks in the eastern Kaili area, are at a highly overmature stage. The amounts of extractable organic matter (EOM) from both solid bitumens and source rocks in the study area were too low for instrumental analysis. Meanwhile, biodegradation and subsequent thermal alteration may influence the characteristics of routine biomarkers in crude oils such as steranes and terpanes (Fang et al., 2011). Unfortunately, most previous research failed to eliminate the influence of such secondary alterations when making bitumen–bitumen correlation studies based on biomarkers in EOM (Ma et al., 2004; Chen et al., 2006; Tian et al., 2006; Ding et al., 2007; Zhang et al., 2007). Thus further direct oil–source correlation study on highly overmature solid bitumen based on biomarkers is needed in the Majiang paleo-reservoir. However, owing to the lack of hydrogen, routine pyrolysis approaches, such as pyrolysis–gas chromatography–mass spectrometry and closed-system thermal maturation cannot release enough biomarkers from high maturity kerogen and solid bitumen.

Catalytic hydropyrolysis (HyPy) may provide a solution to this problem. In HyPy the pyrolysis is assisted by high hydrogen pressure flow and a dispersed sulfided molybdenum catalyst, which permits covalent bond cleavage at relatively low temperature (< 450 °C; Love et al., 1995). Love et al. (1995) first reported that the yields of aliphatic hydrocarbons and covalently bound biomarkers by HyPy were typically higher than that by dichloromethane (DCM) Soxhlet extraction. In recent years, HyPy has been

widely used in the field of petroleum geochemistry (Love et al., 1995, 1998; Zhou et al., 2007; Lockhart et al., 2008; Sun et al., 2008; Liao et al., 2012; Wu et al., 2012). All the previous research (Love et al., 1995; Fang et al., 2012; Liao et al., 2012; Wu et al., 2012, 2013) indicates that the approach has the advantages of maximizing the yields of covalently bonded biomarkers from kerogen, minimizing the structural rearrangement of biomarker species and maintaining the biologically inherited stereochemistry. Thus covalently bound biomarkers released from high maturity kerogen can retain more origin information of organic input than free biomarkers in EOM (Sun et al., 2008). These characteristics make covalently bound biomarkers released by HyPy powerful in tackling the key problems in oil exploration, for example, in severe thermal degradation (Marshall et al., 2007; Zhou et al., 2007; Sun et al., 2008; Fang et al., 2012), severely biodegraded crude oils and tar sand bitumens (Sonibare et al., 2009), and oil-contaminated drill cuttings, where conventional approaches using free biomarkers are limited (Murray et al., 1998; Russell et al., 2004). Liao et al. (2012) altered biodegraded soft bitumen to various maturities by artificial thermal simulation and then HyPy was used to release covalently bound biomarkers from these solid bitumen residues. The Liao et al. (2012) results suggested that the source and maturity related biomarker parameters based on hydropyrolysates are much more stable than those based on common pyrolysates owing to the protection of asphaltene macromolecules, although they have suffered both biodegradation and severe thermal maturation to different extents. Based on this finding, we applied the covalently bound *n*-alkanes and saturated biomarkers released from solid bitumens and source rock kerogens via HyPy to oil–source correlation of the Majiang paleo-reservoir.

2. Samples and experimental

2.1. Samples

Potential source rock and solid bitumens were collected from the frontal zone of the Xuefeng thrust nappe where it is covered with a large area of Paleozoic strata (Fig. 1). The O_1h solid bitumen KLMJ-1 was sampled from the village of Modaoshi in Majiang County and solid bitumen DY-7 was sampled from the town of Bagu in Danzhai County. Carbon-rich rocks were sampled from the Lower Cambrian Niutitang Formation marine mudstones $\in_1$n in Nan'gao and Yangtiaozhai counties, the Lower Silurian Longmaxi Formation (S_1l) and the Lower Permian Qixia Formation (P_1q). The Lower Silurian black shale, formed in a restricted deep shelf, is widely developed in the Upper Yangtze Platform. Neither outcropping nor drilling core samples of S_1l black shale are available in the Majiang area because the outcropping of S_1l black shale mainly occurs in the northwestern part of Guizhou province (Fang et al., 2011) and the Xuefeng thrust nappe, which is east of the Majiang area (Li et al., 2006). The sedimentary facies of the Lower Silurian black shale in the northwestern part of Guizhou province are similar to that in the Xuefeng thrust nappe, which is located in the southeastern part of Guizhou province and the western part of Hunan province, both of restricted deep shelf. Qiu et al. (1994) and Ma et al. (2004) held that the Lower Silurian shale in the Xuefeng thrust nappe is a probable source rock and give evidence from the burial history. Thus, S_1l black shale SW-1 was sampled from Xishui area, to the north of the Majiang paleo-reservoir, to represent S_1l shale of the Xuefeng thrust nappe, which is close to the Majiang paleo-reservoir.

The basic geochemical parameters of the solid bitumens and potential source rocks are listed in Table 1. The $\in_1$n mudstones contain high concentrations of inert carbon suggesting that they had significant source potential. The carbon content in the S_1l shale is lower and is similarly inert. Carbon in the P_1q mudstone still retains some generative potential. The kerogen maceral compositions of the $\in_1$n mudstone samples and the S_1l shale sample are all dominated by micrinite (more than 95%), which was considered to be derived from amorphous material during thermal maturation (Xiao, 1992). Meanwhile, the maceral composition of the P_1q kerogen is dominated by alginate, which indicates marine organic matter input. The solid bitumens yield low amount of pyrolysate, consistent with overmature, but not totally inert, organic carbon. Their bulk $\delta^{13}C$ values are close to those measured for the kerogen in the Lower Cambrian mudstones.

2.2. Experimental

2.2.1. Extractable organic matter (EOM)

The source rocks and solid bitumens were powdered to 80 mesh and Soxhlet extracted using a mixture of DCM and methanol (93:7, v:v) at 46 °C for 72 h. The extracts were treated with *n*-hexane to precipitate asphaltenes and then fractionated on alumina:silica gel (1:3, v:v) columns into saturates, aromatics and resins by successive elution with hexane, hexane:DCM (5:3, v:v), and DCM:MeOH (2:1, v:v), respectively. The contents of EOM in the O_1h solid bitumens and $\in_1$n and S_1l source rocks were all very low (Table 2).

2.2.2. Catalytic hydropyrolysis

HyPy experiments were then performed on all the solid bitumens and kerogens using procedures described in detail in Liao et al. (2012) and Wu et al. (2012, 2013). Briefly, ground solid bitumens and rocks were treated with hydrochloric acid and hydrofluoric acid to remove carbonate and silicate minerals. The solid organic carbon enriched residues were extracted with a mixture of benzene, acetone and methanol (5:5:2, v:v:v) at 72 °C for two weeks to remove residual hydrocarbons and the TOC measured (Table 2). Prior to hydropyrolysis analysis, the bitumens and kerogen enriched rocks were impregnated with an aqueous solution of ammonium dioxydithiomolybdate $[(NH_4)_2MoO_2S_2]$ to give a nominal loading of 5 wt% molybdenum, as described previously by Roberts et al. (1995) and Rocha et al. (1997). Then, the samples were put into the HyPy reactor tube and heated from ambient temperature to 300 °C at 250 °C/min and held at 300 °C for 2 min to further remove adsorbed hydrocarbons. The silica trap was replaced and the reactor tube heated from ambient temperature to 250 °C at 300 °C/min, and then from 250 °C to 520 °C at 8 °C/min, before being finally held at 520 °C for 5 min. The system is maintained under a constant H_2 pressure of 15 MPa and a sweep gas flow of 5 l/min to ensure that all volatile products are quickly removed from the reactor and are collected in the silica trap, which was cooled with liquid nitrogen. Before each pyrolysis, the reactor tube and trap are cleaned, rinsed with DCM, and then heated at 600 °C for 6 h to deplete possible contaminating organic matter. Hydropyrolysates were extracted from the silica using a mixture of DCM and methanol (93:7, v:v) at 46 °C for 72 h and then fractionated into saturates, aromatics, resins and asphaltenes fractions by column chromatography.

2.2.3. Gas chromatography–mass spectrometry and gas chromatography–isotope ratio mass spectrometry

Gas chromatography–mass spectrometry (GC–MS) analysis was conducted on a Finnigan Trace GC Ultra gas chromatograph, equipped with a DB-5 fused silica capillary column (60 m × 0.32 mm i.d. × 0.25 μm film thickness) coupled to a Thermo Fisher DSQ II mass spectrometer. The GC oven was held isothermally at 70 °C for 2 min, programmed to 295 °C at 4 °C/min, with a final hold time of 25 min. The ion source temperature was 250 °C, and the instrument was operated in the electron impact mode with an electronic energy of 70 eV.

Table 1
Basic geochemical parameters of the samples in the Majiang area.

Sample	Formation	Description	R_o (%)	TOC (%)	T_{max} (°C)	HI	Bulk $\delta^{13}C$ (‰)
SW-8	$\in_1$n	Mudstone	2.58	6.44	609	2	−32.5
YT-1	$\in_1$n	Mudstone	2.53	6.81	608	2	−34.6
SW-1	S_1l	Shale	2.61	1.49	608	1	−29.2
WC-3	P_1q	Mudstone	0.67	2.01	449	130	−27.5
KLMJ-1	O_1h	Solid bitumen	–	–	467	70	−32.3
DY-7	O_1h	Solid bitumen	2.1	–	528	51	−31.9

Table 2
Yields of EOM by Soxhlet and hydropyrolysates by HyPy.

Sample	TOC of kerogen or bitumen (%)	EOM (mg/g TOC)	Yield of HyPy (mg/g TOC)	EOM/HyPy
SW-8	37.2	0.3	13.4	44.6
YT-1	43.8	0.5	20.6	39.4
SW-1	10.7	5.4	28.2	5.3
WC-3	53.1	81.6	463.5	5.7
KLMJ-1	58.1	0.4	182.5	456
DY-7	86.3	0.8	19.7	25.7

Normal alkanes were separated from the saturated hydrocarbon by urea adduction prior to the gas chromatography–combustion–isotope ratio mass spectrometry (GC–C–IRMS) analysis to improve measurement precision. The details of the urea adduction and GC–C–IRMS analysis are described by Liao et al. (2004, 2009). Briefly, GC–C–IRMS analyses were performed in a VG Isochrom II system. The GC was fitted with a 30 m × 0.32 mm × 0.25 μm i.d. DB-1 fused silica capillary column. The GC was held at 70 °C for 2 min, programmed to 295 °C at 4 °C/min, and then kept at 295 °C for 25 min. The combustion furnace was held at 850 °C. Carbon isotope ratios were measured relative to a CO_2 reference gas introduced at the beginning and end of each analysis, and reported relative to the Vienna Pee Dee Belemnite standard. *n*-Alkane standards of known $\delta^{13}C$ were measured every several samples to monitor the precision of the measurement. The standard deviation of the GC–C–IRMS measurement for each compound is typically < 0.2‰. Every sample was measured at least twice.

3. Results and discussion

Table 2 lists the amount of EOM from the samples and the total yields of hydropyrolysates released from the solid bitumens and kerogens. The amount of EOM is lower than 1.0 mg/g TOC for all samples except WC-3 and SW-1. It is well known that the amount of EOM from highly overmature solid bitumens and source rocks is very low owing to severe thermal decomposition and condensation of organic matter. However, the total yields of the hydropyrolysates are 6–40 times greater than those of the extracts (Table 2). Previous research has also shown that the total yields of HyPy hydropyrolysates were higher than the corresponding EOM by Soxhlet extraction, especially at the highly overmature stage (Zhou et al., 2006; Liao et al., 2012; Wu et al., 2013). The characteristics of biomarkers in EOM and hydropyrolysates from both potential source rocks and solid bitumen are shown and compared below. Oil–source correlations are made based on covalently bound biomarkers released by HyPy and isotopic data.

3.1. Comparison of biomarkers in EOM and the corresponding hydropyrolysates

3.1.1. Potential source rocks

The GC–MS total ion chromatograms of saturated hydrocarbon fractions of the EOM from both potential source rocks and solid bitumens are shown in Fig. 2. *n*-Alkanes were detected in the EOM of all source rocks. The carbon numbers of *n*-alkanes of high maturity source rocks YT-1, SW-8, and SW-1 range from 14–26, 16–29, and 14–23, respectively. Meanwhile, the low maturity Permian source rock WC-3 exhibited a more complete *n*-alkane distribution, with carbon numbers ranging from 14–32.

Fig. 3 shows the *m*/*z* 191 and 217 mass chromatograms from GC–MS analysis of the saturate fractions of both the EOM and the hydropyrolysates. The distributions of both terpanes and steranes in the EOM are different from those of hydropyrolysates. As the biomarkers in the hydropyrolysates were liberated from the solid organic matrix they provide a better means of correlation as it is not certain that the free biomarkers in the EOM are syngenetic.

The distributions of C_{27}–C_{29} ααα*R* steranes are widely used in oil–source correlations (Moldowan et al., 1985; Peters and Moldowan, 1993; Czochanska et al., 1988). The distributions of C_{27}–C_{28}–C_{29} ααα*R* steranes in the EOM of $\in_1$n mudstones SW-8 and YT-1 exhibit a similar C_{27} predominance ($C_{27} > C_{29} \geqslant C_{28}$) (Table 3), whereas for the kerogen hydropyrolysates, the distributions of C_{27}–C_{28}–C_{29} ααα*R* steranes of SW-8 and YT-1 exhibit similar $C_{27} \approx C_{29} > C_{28}$ shape. The distribution of C_{27}–C_{28}–C_{29} ααα*R* steranes in the EOM of S_1l shale exhibits a C_{27} predominance ($C_{27} > C_{29} > C_{28}$) whereas that in the corresponding hydropyrolysates are enriched in C_{29} ($C_{29} > C_{27} \approx C_{28}$). The distribution of C_{27}–C_{28}–C_{29} ααα*R* steranes in both EOM and hydropyrolysates of P_1q mudstone WC-3 exhibits a similar C_{29} predominance ($C_{29} > C_{27} \approx C_{28}$).

The ratios of C_{29} norhopane to C_{30} hopane (H_{29}/H_{30}), gammacerane to C_{30} hopane (Gam/H_{30}), and C_{23} tricyclic terpane to C_{24} tricyclic terpane (TT_{23}/TT_{24}) are common source related parameters (Peters et al., 2005; Liao et al., 2012). The H_{29}/H_{30} ratios in EOM of both potential source rocks and solid bitumens are rather similar, with all in the range of 0.5–0.59. For hydropyrolysates, the H_{29}/H_{30} ratios of Lower Silurian source rock SW-1 and Lower Permian source rock WC-3 are 0.49 and 0.41, respectively. However, the H_{29}/H_{30} ratios in hydropyrolysates of Lower Cambrian source rock YT-1 and SW-8 are 0.61 and 0.59, respectively. In brief, the H_{29}/H_{30} ratios in hydropyrolysates exhibit more significant differences between the Lower Cambrian source rocks and other source rocks than the differences indicated by EOM, indicating significant differences in organic input of source rocks.

Gammacerane indicates a stratified water column in marine and non-marine source rock depositional environments (Sinninghe

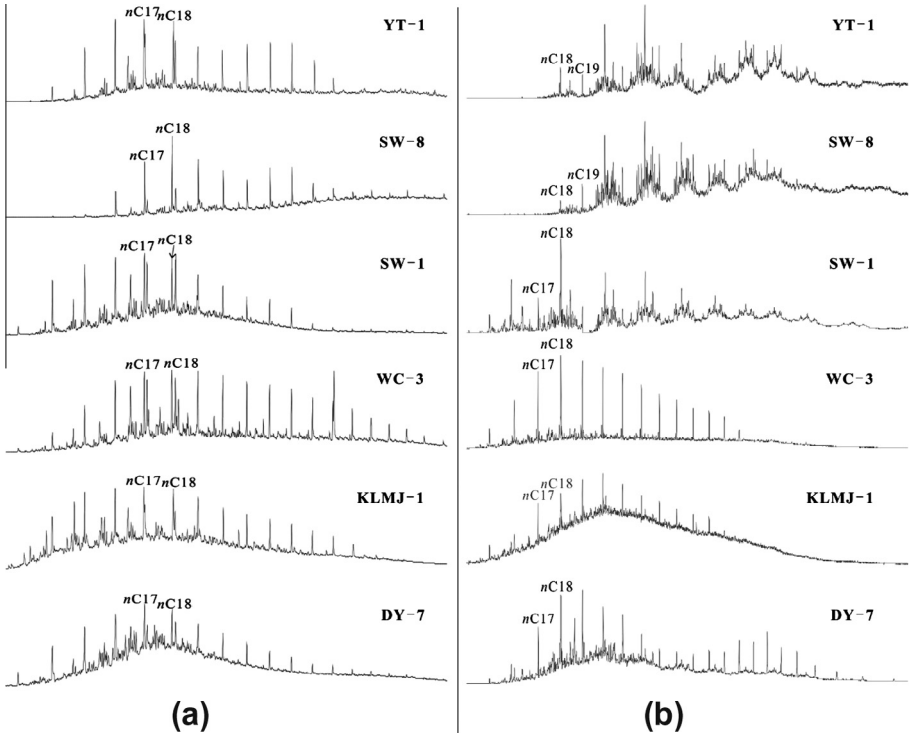

Fig. 2. Total ion chromatograms of saturated hydrocarbon fractions in (a) the Soxhlet extracts and (b) the hydropyrolysates. *n*C17 = C_{17} normal paraffin hydrocarbon; *n*C18 = C_{18} normal paraffin hydrocarbon.

Damsté et al., 1995), and this is commonly considered to result from hypersalinity at depth (Peters et al., 2005). The Gam/H_{30} ratios in the EOM range from 0.05–0.16, but the ratio of SW-8 cannot be calculated owing to the low abundance (Table 3). Gammacerane was detected in the hydropyrolysates of all four source rock samples and the Gam/H_{30} ratios are very similar, all in the range of 0.14–0.18 (Table 3). This is consistent with the fact that the four potential source rock samples were all deposited in a marine depositional environment.

Through a simulation study, the $TT_{23}/(TT_{23}+TT_{24})$ ratio also proved to be a reliable index in bitumen–source and bitumen–bitumen correlations for solid bitumens that have suffered heavy biodegradation and subsequent severe thermal alteration (Liao et al., 2012). The $TT_{23}/(TT_{23}+TT_{24})$ ratio of Lower Silurian source rock is highest of all source rocks, with a value of 2.46. The $TT_{23}/(TT_{23}+TT_{24})$ ratio of Lower Permian source rock sample WC-3 is lowest of all, with a value of 1.52. $TT_{23}/(TT_{23}+TT_{24})$ ratios in the EOM of Lower Cambrian source rock samples YT-1 and SW-8 are 1.64 and 1.73, respectively. For kerogen hydropyrolysates, SW-1 still exhibits the highest value of 2.65, and WC-3 has the lowest value of 1.3, while Lower Cambrian source rocks YT-1 and SW-8 have moderate values of 2.3 and 1.8, respectively. Therefore, $TT_{23}/(TT_{23}+TT_{24})$ ratios in both EOM and hydropyrolysates from various strata indicate significant differences. Differences in all source-related biomarker parameters discussed above can be all attributed to the differences in organic input and depositional environment.

Commonly used biomarker maturation parameters are compared in Table 3. The 22S/(22S + 22R) homohopane isomerization ratios for C_{31}–C_{35} hopanes are specific for immature to early oil generation stages, (Peters et al., 2005) and are at equilibrium for the extracts and hydropyrolysates. These results are consistent with previous observations that there are no significant difference between the 22S/(22S + 22R) isomerization ratios of $C_{31}\alpha\beta$ homohopane in the extracts and hydropyrolysates of high maturity source rocks (T_{max} > 460 °C) with Type II kerogen (Lockhart et al., 2008) and solid bitumen (Liao et al., 2012). The Ts/(Ts + Tm) ratio is dependent on maturity, although it may also be affected by the depositional environment (Peters et al., 2005). Ts/(Ts + Tm) ratios in both EOM and hydropyrolysates are similar, ranging from 0.50–0.56, which is consistent with the high maturities of these samples.

The C_{29} sterane isomer ratios of C_{29} 20S/(20S + 20R) and C_{29} ββ/(ββ + αα) are often used as maturity indicators for crude oils. The equilibrium end point of the C_{29} 20S/(20S + 20R) ratio is in the range of 0.52–0.55 (Peters et al., 2005). EOM C_{29}-20S/(20S + 20R) ratios are in the range of 0.42–0.58 (Table 3 and Fig. 4), which is very close to its end point. However, C_{29}-20S/(20S + 20R) ratios in hydropyrolysates are in the range of 0.29–0.34, which is much lower than those in their corresponding EOM (0.42–0.58) (Fig. 4). C_{29} ββ/(ββ + αα) ratios increase with higher thermal maturity and reach the end point in the range of 0.61–0.70 (Peters et al., 2005). C_{29} ββ/(ββ + αα) ratios in the hydropyrolysates are all in the range of 0.39–0.44, similar to those in the corresponding EOM (which lie in the range of 0.37–0.46).

The above comparisons indicate that C_{29}-20S/(20S + 20R) ratios based on isomerization of covalently bound C_{29} sterane are generally less mature than that in the corresponding EOM. However, similar to other commonly used maturity parameters in EOM, parameters such as C_{29} sterane isomerization ratios of C_{29} ββ/(ββ + αα), C_{31}-homohopane ratios (C_{31}-22S/(22S + 22R)), and the Ts/(Ts + Tm) ratio based on covalently bound C_{29} sterane all reach their end points at a highly overmature stage. Murray et al. (1998) indicated that the covalently bound hopanes and steranes undergo the same epimerization reaction pathways as their free counterparts in the bitumen, but they are generally less mature in terms of isomerization at both ring and side-chain chiral centers.

3.1.2. O_1h solid bitumens

n-Alkanes were detected in the EOM of the two solid bitumens KLMJ-1 and DY-7 (Fig. 2). The carbon numbers of *n*-alkanes range from C_{13-29} and coelute with an unresolved complex mixture

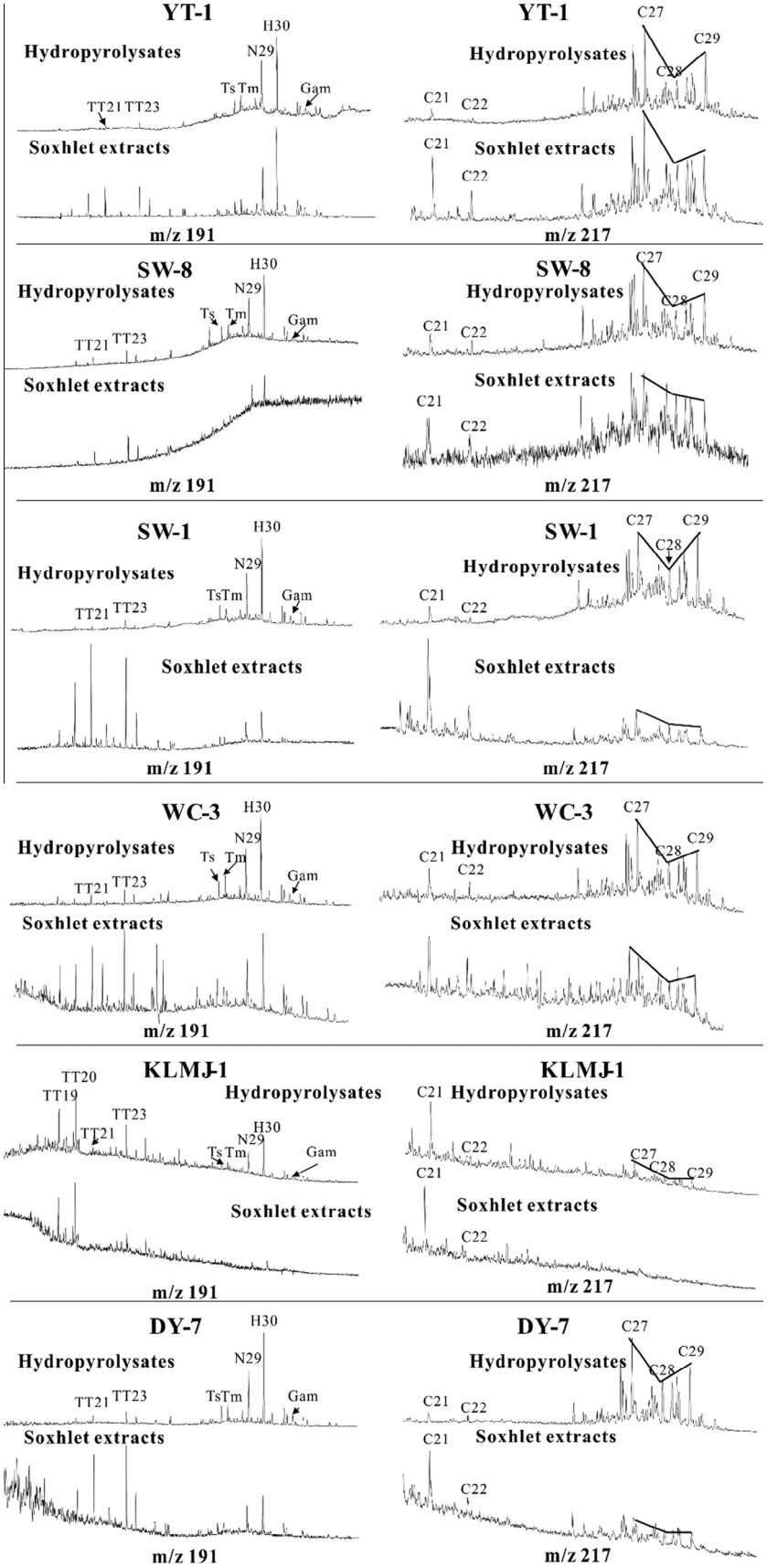

Fig. 3. *m*/*z* 191 and *m*/*z* 217 mass chromatograms of Soxhlet extracts and hydropyrolysates of source rocks and solid bitumens. TT19–24 = C_{19-24} tricyclic terpanes; Ts = C_{27} 18α(H) trisnorhopane; Tm = C_{27} 17α (H) trisnorhopane; H29–30 = C_{29-30} 17α(H) 21β(H) hopanes; Gam = gammacerane; C21 = Pregnane; C22 = Homopregnane; C27 = C27 ααα20R cholestane; C28 = C_{28} ααα20R ergostane; C29 = C_{29} ααα20R stigmastane.

Table 3
Biomarker parameters in Soxhlet extracts and hydropyrolysates.

Biomarker parameter	Extracts						Hydropyrolysis products					
	Source rocks				Bitumens		Source rocks				Bitumens	
	SW-1	WC-3	YT-1	SW-8	KLMJ-1	DY-7	SW-1	WC-3	YT-1	SW-8	KLMJ-1	DY-7
22S/(22S + 22R) C_{31}-homohopane	0.65	0.63	0.56	–	–	0.6	0.58	0.56	0.6	0.59	0.59	0.59
22S/(22S + 22R) C_{29}-sterane	0.42	0.5	0.55	0.58	–	0.48	0.29	0.34	0.32	0.32	0.36	0.38
ββ/(ββ + αα) C_{29}-sterane	0.39	0.37	0.42	0.46	–	0.51	0.39	0.44	0.41	0.41	0.41	0.39
Ts/(Ts + Tm)	0.51	0.56	0.51	0.51	–	0.47	0.54	0.50	0.51	0.55	0.54	0.55
C_{27}/C_{27}–C_{29} ααα*R* sterane	0.43	0.31	0.40	0.46	–	0.41	0.28	0.31	0.38	0.38	0.38	0.37
C_{28}/C_{27}–C_{29} ααα*R* sterane	0.27	0.32	0.28	0.27	–	0.29	0.27	0.31	0.27	0.27	0.25	0.28
C_{29}/C_{27}–C_{29} ααα*R* sterane	0.30	0.37	0.32	0.27	–	0.3	0.46	0.38	0.36	0.36	0.37	0.35
C_{21}/C_{22}	2.28	1.51	2.05	1.97	5.21	2.38	2.21	1.48	1.89	1.78	2.91	1.90
H_{29}/H_{30}	0.5	0.53	0.58	0.58	0.59	0.56	0.49	0.41	0.61	0.59	0.62	0.64
Gam/H30	0.05	0.16	0.1	–	–	–	0.16	0.18	0.16	0.14	0.19	0.20
TT_{23}/TT_{24}	2.46	1.52	1.64	1.73	–	2.41	2.65	1.3	2.3	1.8	2.0	1.9

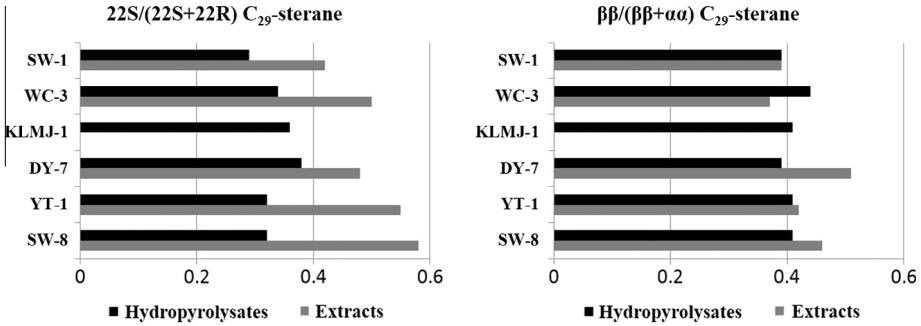

Fig. 4. Maturity parameters of the extracts and the hydropyrolysates.

(Fig. 2). In the EOM of KLMJ-1, pregnane and homopregnane are dominant steranes in the mass chromatograms of *m*/*z* 217, but C_{27}–C_{29} ααα*R* steranes are almost absent. Tricyclic terpanes are the dominant terpanes in the mass chromatograms of *m*/*z* 191 in the EOM and most pentacyclic terpanes are not detected except for C_{29} and C_{30} hopanes (Fig. 3). The low concentrations of C_{27}–C_{29} ααα*R* steranes and pentacyclic terpanes in EOM of both DY-7 and KLMJ-1 may be attributed to severe biodegradation. It is widely accepted that pregnane and homopregnane have higher bioresistance than C_{27}–C_{29} ααα*R* steranes, and tricyclic terpanes have higher bioresistance than hopanes (Peters et al., 2005). Previous studies revealed that the oil seepages in the Ordovician–Silurian reservoir of the Majiang paleo-reservoir have experienced severe biodegradation, above rank 9 on the Peters and Moldowan scale (abbreviated as the PM level in following; Peters and Moldowan, 1993), during tectonic uplift (Fang et al., 2011) ahead of thermal maturation at deep burial depth (Xue et al., 2007), resulting in severe alteration on both tricyclic and pentacyclic terpanes. Therefore, the presence of *n*-alkanes and the absence of C_{27}–C_{29} ααα*R* steranes in EOM of KLMJ-1 (relative abundance of C_{27}–C_{29} ααα*R* steranes are also extremely low in EOM of DY-7) should be the result of thermal cracking of severely biodegraded bitumens during subsequent thermal maturation. However, higher concentrations of covalently bound hopanes and C_{27}–C_{29} regular steranes were released from bitumens DY-7 and KLMJ-1 by HyPy relative to the corresponding EOM, so establishing an oil–source correlation between highly overmature solid bitumens and potential source rocks based on the covalently bound biomarkers is possible. The distribution of C_{27}–C_{29} ααα*R* steranes in the EOM of bitumen DY-7 exhibits the shape of $C_{27} > C_{29} \approx C_{28}$. However, for the hydropyrolysates in both KLMJ-1 and DY-7, the distributions of C_{27}–C_{29} ααα*R* steranes exhibit a similar shape of $C_{27} > C_{29} > C_{28}$ (Fig. 3 and Table 3). The H_{29}/H_{30} ratios in the EOM of solid bitumens KLMJ-1 and DY-7 are 0.59 and 0.56, which are very similar to those in the corresponding hydropyrolysates, whose values are 0.62 and 0.64, respectively. The Gam/H_{30} ratio in the extracts from solid bitumens KLMJ-1 and DY-7 cannot be calculated owing to their low EOM contents and low concentration in gammacerane (Table 3). However, the Gam/H_{30} ratios in the hydropyrolysates of solid bitumens KLMJ-1 and DY-7 are similar, with values of 0.19 and 0.20, respectively.

Briefly, the source related biomarker parameters such as the distribution of C_{27}–C_{28}–C_{29} ααα*R* steranes and the ratios of H_{29}/H_{30} and Gam/H_{30} in the EOM of both solid bitumens and potential source rocks in the study area indicate that free biomarkers were significantly altered by severe biodegradation and/or thermal maturation. However, the covalently bound biomarkers show higher resistance to such secondary alterations. This may be due to the protection of the geo-macromolecular structure (Rubinstein et al., 1979; Cassani and Eglinton, 1986; Love et al., 1995, 1998; Russell et al., 2004; Lockhart et al., 2008) and generation under high hydrogen pressure and rapid product transport and quenching of the HyPy system (Liao et al., 2012). Therefore, despite their severe secondary alterations, the covalently bound biomarkers released from these solid bitumens can represent origin geochemical information, such as the organic matter input and paleo-sedimentary environment.

3.2. Oil–source correlations

3.2.1. Regular steranes

The distribution of C_{27}–C_{28}–C_{29} ααα*R* steranes in the O_1h bitumen DY-7 EOM correlates to those found in the Lower Silurian shale and the Lower Cambrian marine mudstones but not the Permian mudstone (Fig. 5). The abundance of C_{27}–C_{28}–C_{29} ααα*R* steranes in the EOM of KLMJ-1 is too low to calculate their distribution. As mentioned above, biomarkers in the source rock extracts may have been thermally altered; consequently, their reliability is

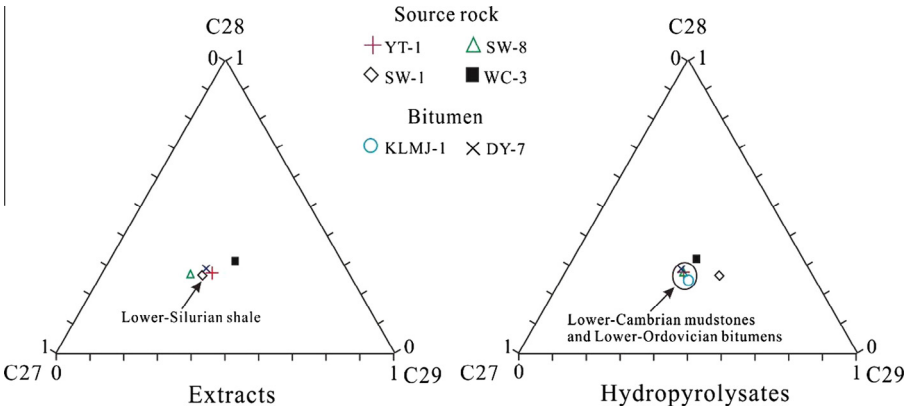

Fig. 5. Triangular plot of the distribution of C_{27}, C_{28}, and C_{29} ααα*R* regular steranes in the Soxhlet extracts and the hydropyrolysates of source rocks and solid bitumens.

questionable. Therefore, the distributions of steranes in hydropyrolysates may be more reliable indicators for source correlation (Fig. 5). The distributions of C_{27}–C_{28}–C_{29} ααα*R* steranes in the hydropyrolysates of the O_1h bitumens are quite similar to those of $\in_1n$ marine mudstones but significantly different from those in P_1q and S_1l source rocks.

The pregnane/homopregnane ratios (C_{21}/C_{22}) in the EOM are very similar to those in the corresponding hydropyrolysates. However, in the EOM of the solid bitumens the C_{21}/C_{22} ratios are much higher than those in the corresponding hydropyrolysates. Multiple processes influence this ratio. Pregnanes are derived from the hormones pregnanol and pregnanone and high concentrations of pregnane and homopregnane may indicate a hypersaline depositional environment (Huang et al., 1984; De Leeuw and Bass, 1986). Pregnanes also may be produced by thermal cracking of C_{27}–C_{29} regular steranes during thermal maturation (Huang et al., 1994). Pregnane and homopregnane have the highest bioresistance in steranes because the biodegradation of the C_{20} and C_{21} steranes is limited to enzymatic attack of the core structure owing to the absence of an alkyl substituent at C-17 and may be unaltered up to PM level 8 (Peters et al., 2005). At the most severe levels of biodegradation, the ratio may be altered as homopregnane may have lower bioresistance because it has one more methyl group than pregnane. Hence, the higher C_{21}/C_{22} ratios in the EOM of the solid bitumens may be attributed to severe biodegradation. Furthermore, the high C_{21}/C_{22} ratio and low relative concentrations in both pentacyclic terpanes and C_{27}–C_{29} regular steranes within the hydropyrolysates of KLMJ-1 may also indicate that the covalently bound biomarkers were altered to some extent at an extremely severe biodegradation stage. Nevertheless, the C_{21}/C_{22} ratio in the hydropyrolysates of DY-7 is very close to those in the hydropyrolysates of from the Lower Cambrian source rocks.

3.2.2. Tricyclic and pentacyclic terpanes

The H_{29}/H_{30} ratio is commonly used as a source related biomarker parameter for oil–source correlation (Peters et al., 2005; Liao et al., 2012). The H_{29}/H_{30} ratio in the EOM of DY-7 is significantly higher than that in the EOM of DY-7, perhaps as a result of C_{29} hopane being more resistant to thermal alteration than C_{30} hopane, leading to an increase in the H_{29}/H_{30} ratio with thermal maturity (Peters et al., 2005). The T_{max} values of the two O_1h bitumens indicate that the maturity of DY-7 is higher than that of KLMJ-1 (Table 1). However, the H_{29}/H_{30} ratios of the hydropyrolysates in the two O_1h solid bitumens are very close to the H_{29}/H_{30} ratios in the hydropyrolysates of the two Lower Cambrian marine mudstones and significantly higher than those seen in the hydropyrolysates of the Silurian and Lower Permian mudstones (Table 3 and Fig. 6). Similarly, the TT_{23}/TT_{24} ratios in the hydropyrolysates of the O_1h solid bitumens are closest to those measured in the hydropyrolysates of the two Lower Cambrian mudstones and farthest from the Silurian and Lower Permian mudstones. Collectively, the hydropyrolysates from O_1h solid bitumens correlated best to the Lower Cambrian marine mudstones.

3.2.3. $\delta^{13}C$ values of bulk kerogens (solid bitumens) and individual *n*-alkanes in hydropyrolysates

The $\delta^{13}C$ of kerogens of the Lower Cambrian mudstones and solid bitumens are significantly lighter than the kerogens in the Silurian and Lower Permian rocks (Table 1). The kerogen values are consistent with temporal effects and suggest that the O_1h solid bitumens could be derived from the Lower Cambrian marine mudstones.

The stable carbon isotopic compositions of individual *n*-alkanes are useful tools in oil–oil and oil–source correlation (Bjorøy et al., 1991). Because of the high maturity, the concentrations of *n*-alkanes in the extracts of Lower Cambrian mudstone SW-8 and Lower Ordovician bitumen DY-7 are too low to measure their isotopic values. However, the concentrations of *n*-alkanes in the hydropyrolysates were high enough to measure. Fig. 7 shows the $\delta^{13}C$ distributions of the individual *n*-alkanes in the hydropyrolysates of kerogens and solid bitumens, together with the EOM of the bitumen KLMJ-1. The $\delta^{13}C$ values of the individual *n*-alkanes in the hydropyrolysates of Lower Cambrian mudstones YT-1 and SW-8 are in the range of −29‰ to −32‰; these values are quite similar to those in the hydropyrolysates of the Lower Silurian shale SW-1 but quite different from those in the hydropyrolysates of the Lower Permian mudstone WC-3 (Fig. 7). The $\delta^{13}C$ values of individual *n*-alkanes from the hydropyrolysates of the two O_1h bitumens are in the range of −27.5‰ to −31.4‰ and −29.8‰ to −33.6‰, respectively, which are much closer to those in the hydropyrolysates of Lower Cambrian mudstones than in the hydropyrolysates of the Lower Permian mudstone. As mentioned above, KLMJ-1 may have suffered severe biodegradation above PM level 9 but there exists a complete distribution of *n*-alkanes in the EOM. The $\delta^{13}C$ values of individual *n*-alkanes in the EOM and the hydropyrolysates of the bitumen KLMJ-1 are close to each other. Thus, the *n*-alkanes in the severely biodegraded bitumen KLMJ-1 were most likely generated from thermal cracking of the biodegraded bitumen. However, the possibility of the reservoir being charged by non-biodegraded oil from the same source rock can be excluded because of the extremely low relative concentrations (or absence) of C_{27}–C_{29} regular steranes and pentacyclic in EOM.

By taking the source related biomarker parameters above, the $\delta^{13}C$ distribution of the covalently bound *n*-alkanes, and the bulk $\delta^{13}C$ values of kerogens and bitumens into account, we conclude that the O_1h bitumens were generated from the Lower Cambrian

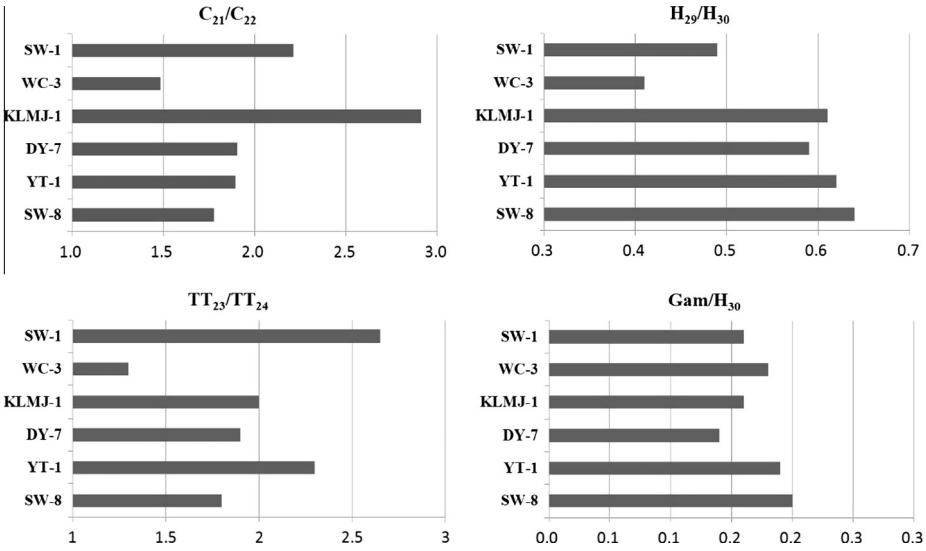

Fig. 6. Source-specific parameters of the hydropyrolysates.

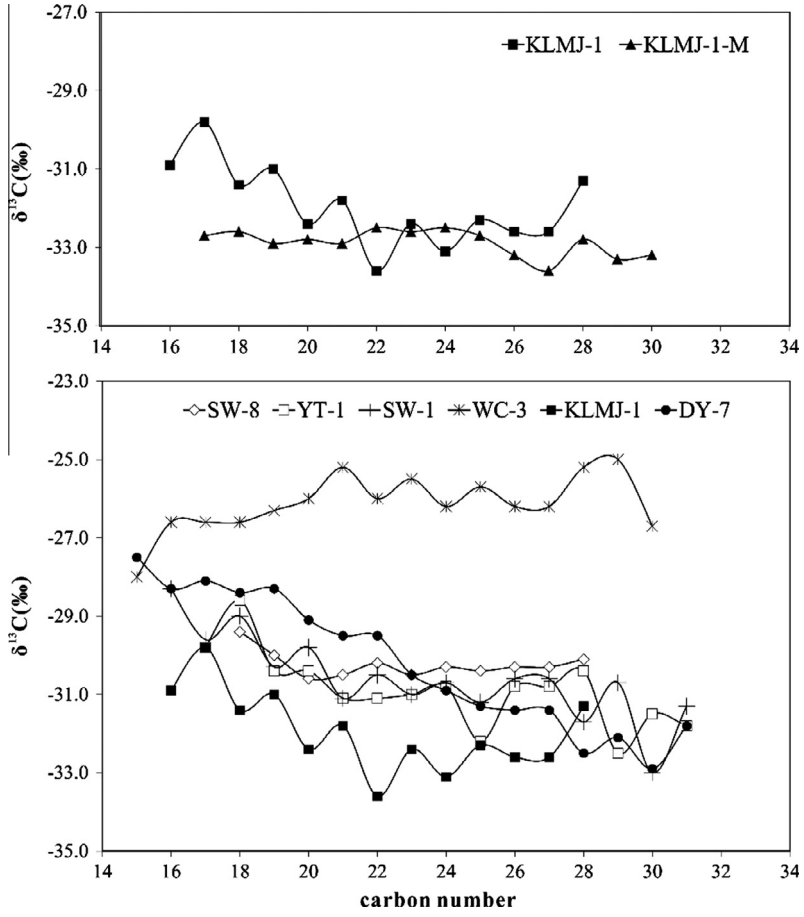

Fig. 7. $\delta^{13}C$ values of *n*-alkanes in hydropyrolysates. KLMJ-1-M: extracts of KLMJ-1.

mudstones. This conclusion is consistent with the conclusions of Fang et al. (2011) based on the distributions of dimethyldiamantanes and triaromatic steroid hydrocarbons in EOM together with bulk $\delta^{13}C$. It also suggests that the covalently bound biomarkers released by HyPy can provide dependable information for the oil–source correlation in the Majiang paleo-reservoir.

3.3. The evolution of the Majiang paleo-reservoir

The characteristics of both the EOMs and the hydropyrolysates from solid bitumen KLMJ-1 suggest that it suffered severe biodegradation before thermal alteration. In fact, the differences in the geochemical characteristics between bitumens DY-7 and

KLMJ-1 can be attributed to the differences in their structural location and also burial history. Modeling indicates that during the Late Caledonian period, the Majiang paleo-reservoir was charged by the oil generated from the Lower Cambrian mudstones and erosion of caprock for the Majiang paleo-reservoir were reported to have occurred during the Caledonian period (Wu, 1989; Tenger et al., 2008). Since KLMJ-1 was located at the Majiang anticlinal nucleus, the capping strata were easily eroded (Wang et al., 1997). As a consequence, the oil reservoir at the Majiang anticlinal nucleus where KLMJ-1 is located suffered severe evaporation and biodegradation during the Late Caledonian period. In contrast, the capping strata of the paleo-reservoir in the Danzhai area where DY-7 is located were not eroded. Thus, bitumen DY-7 has not suffered biodegradation (if DY-7 is biodegraded) as severe as KLMJ-1 during the Caledonian period. After the Late Caledonian, the burial depth of the O_1h paleo-reservoir in the Majiang area increased continuously, as indicated by evidence from structural evolution, geochemistry, and fluid inclusion homogenization temperature research (Xiang et al., 2008; Chen et al., 2010; Fang et al., 2011). As a consequence, the bitumens in the reservoir suffered thermal alteration to various extents. Because of bitumen DY-7's deeper burial depth, its maturity was much higher than that of bitumen KLMJ-1. The abundant heavy fractions in the biodegraded bitumens released light oil at higher maturity. This provides a reasonable explanation to the phenomenon that there exist dominant *n*-alkanes in the chromatograms of the EOMs of KLMJ-1 and DY-7 whereas regular steranes and hopanes were absent in KLMJ-1 and of low relative abundances in DY-7. Furthermore, the $\delta^{13}C$ values of *n*-alkanes in the EOM of KLMJ-1 (Fang et al., 2011) were quite similar to those of covalently bound *n*-alkanes, providing further evidence that the *n*-alkanes in EOM have an origin identical to that of the hydropyrolysates. Due to continuous uplift, the Majiang paleo-reservoir was finally destroyed between the Late Yanshanian period and the Early Himalayan period (namely, from the Cretaceous to the Early Cenozoic) (Xiang et al., 2008). This result was also supported by Re–Os isotope system dating of bitumen in the Majiang paleo-reservoir (Chen et al., 2010).

4. Conclusion

Based on a comparison of isotopic data on the yields and biomarkers obtained by Soxhlet extraction and catalytic hydropyrolysis, the following conclusion can be made. Covalently bound biomarkers released by catalytic hydropyrolysis are more stable than free biomarkers in the EOM despite the presence of severe secondary alterations. Covalently bound biomarkers can provide more dependable information for oil–source correlation if the kerogens and solid bitumens are all of high maturity. The O_1h solid bitumens of the Majiang paleo-reservoir were generated from the Lower Cambrian mudstones. O_1h bitumen in the Majiang anticline suffered severe biodegradation ahead of thermal alteration where as those in the Danzhai area did not.

Acknowledgments

This work was supported by the National Science and Technology Major Project (Grant Nos. 2011ZX05008-002 and 2011ZX05005-001), the National Natural Science Foundation of China (Grant No. 40739902), and GIGCAS 135 Project No. Y234021001. This is contribution No. IS-1810 from GIGCAS. We are grateful to Prof. Wenhui Liu, Dr. Tenger and Dr. Jie Wang of Sinopec and Prof. Yongge Sun of Zhejiang University for useful suggestions and other help, and Mr. Huashan Chen of Guangzhou Institute of Geochemistry for help in GC–C–IRMS analysis. Dr. Colin E. Snape and Dr. Haiping Huang are gratefully acknowledged for their constructive comments and suggestions. We are indebted to Dr. Clifford C. Walters for his useful suggestions and patience in handling the paper.

Associate Editor—**Cliff Walters**

References

Bjorøy, M., Hall, K., Gillyon, P., Jumeau, J., 1991. Carbon isotope variations in *n*-alkanes and isoprenoids of whole oils. Chemical Geology 93, 13–20.

Cassani, F., Eglinton, G., 1986. Organic geochemistry of Venezuelan extra-heavy oils, 1. Pyrolysis of asphaltenes: a technique for the correlation and maturity evaluation of crude oils. Chemical Geology 56, 167–183.

Chen, L., Ma, C., Lin, W., She, Z., Chen, Z., 2010. Indosinian hydrocarbon accumulation in South China: A Re-Os isotope constrain. Geological Science and Technology Information 29, 95–99.

Chen, Y., Zhang, H., Li, X., Chu, L., Zhang, W., Deng, W., Huang, C., 2006. Sedimentary and structural evolution and oil–gas exploration direction in Jiangnan-Xuefeng structural belt and its edge. South China Oil & Gas 72, 5–10 (in Chinese with English abstract).

Czochanska, Z., Gilbert, T.D., Philp, R.P., Sheppard, C., Weston, R.J., Wood, T.A., Woolhouse, A.D., 1988. Geochemical application of sterane and triterpane biomarkers to a description of oils from the Taranaki Basin in New Zealand. Organic Geochemistry 12, 123–135.

De Leeuw, J.W., Bass, M., 1986. Early diagenesis of steroids. In: Johns, R.B. (Ed.), Biological Markers in the Sedimentary Record. Elsevier, Amsterdam, pp. 102–127.

Ding, D., Liu, G., Chen, Y., Pan, W., Qu, C., Rao, D., 2007. Hydrocarbon accumulation and oil–source correlation in the front of Jiangnan-Xuefeng mountain: series 3 of the southern structure studies. Petroleum Geology & Experiment 29, 345–354 (in Chinese with English abstract).

Fang, Y., Liao, Y., Wu, L., Geng, A., 2011. Oil–source correlation for the paleo-reservoir in the Majiang area and remnant reservoir in the Kaili area, South China. Journal of Asian Earth Sciences 41, 147–158.

Fang, Y., Geng, A., Liao, Y., Wu, L., 2012. Application of catalytic hydropyrolysis in solid oil–source correlation of the paleo-oil reservoirs in Nandan area. Geochimica 41, 122–130 (in Chinese with English abstract).

Hu, Y., Han, R., Mao, X., 2007. Relationship between metal mineralization and accumulation of oil and gas in the eastern Guizhou. Geology and Prospecting 43, 51–56 (in Chinese with English abstract).

Huang, D., Li, J., Zhou, Z., Gu, X., Zhang, D., 1984. Evolution and Hydrocarbon-Generating Mechanism and Non-marine Organic Matter. Petroleum Industry Press, Beijing.

Huang, D., Zhang, D., Li, J., 1994. The origin of 4-methyl steranes and pregnanes from Tertiary strata in the Qaidam Basin, China. Organic Geochemistry 22, 343–348.

Li, C., Wu, Z., Zhang, Z., Chen, G., 2003. The Study of Paleo-reservoir and Remnant Reservoir in the Southern Guizhou Depression of China. Report from Sinopec Exploration Southern Company, pp. 35–38 (in Chinese).

Li, Z., Luo, Z., Liu, S., Yong, Z., 2006. Assessment of petroleum resources in Lower Assemblage (Z-S) under Xuefeng thrust nappe. Oil & Gas Geology 27, 392–398 (in Chinese with English abstract).

Liao, Y., Geng, A., Xiong, Y., Liu, D., Lu, J., Liu, J., Zhang, H., Geng, X., 2004. The influence of hydrocarbon expulsion on carbon isotopic compositions of individual *n*-alkanes in pyrolysates of selected terrestrial kerogens. Organic Geochemistry 35, 1479–1488.

Liao, Y., Geng, A., Huang, H., 2009. The influence of biodegradation on resins and asphaltenes in the Liaohe Basin. Organic Geochemistry 40, 312–320.

Liao, Y., Fang, Y., Wu, L., Geng, A., Hsu, S.C., 2012. The characteristics of the biomarkers and $\delta^{13}C$ of *n*-alkanes released from thermally altered solid bitumens at various maturities by catalytic hydropyrolysis. Organic Geochemistry 46, 56–65.

Lockhart, R.S., Meredith, W., Love, G.D., Snape, C.E., 2008. Release of bound aliphatic biomarkers via hydropyrolysis from Type II kerogen at high maturity. Organic Geochemistry 39, 1119–1124.

Love, G.D., Snape, C.E., Carr, A.D., Houghton, R.C., 1995. Release of covalently-bound alkane biomarkers in high yields from kerogen via catalytic hydropyrolysis. Organic Geochemistry 23, 981–986.

Love, G.D., Snape, C.E., Fallick, A.E., 1998. Differences in the mode of incorporation and biogenicity of the principle aliphatic constituents of a Type I oil shale. Organic Geochemistry 28, 797–811.

Ma, L., Chen, H., Gan, K., Xu, K., Xu, X., Wu, G., Ye, Z., Liang, X., Wu, S., Qu, Y., Zhang, P., Ge, P., 2004. Geotectonics and Petroleum Geology of Marine Sedimentary Rocks in Southern China. Geological Publishing House, Beijing, China, pp. 455–566.

Marshall, C.P., Love, G.D., Snape, C.E., Hill, A.C., Allwood, A.C., Walter, M.R., Kranendonk, M.J.V., Bowden, S.A., Sylv, S.P., Summons, R.E., 2007. Structural characterization of kerogen in 3.4 Ga Archaean cherts from the Pilbara Craton, Western Australia. Precambrian Research 155, 1–23.

Moldowan, J.M., Seifert, W.K., Gallegos, E.J., 1985. Relationship between petroleum composition and depositional environment of petroleum source rock. American Association of Petroleum Geologists Bulletin 69, 1255–1268.

Murray, I.P., Love, G.D., Snape, C.E., Bailey, N.J.L., 1998. Comparison of covalently bound aliphatic biomarkers released via hydropyrolysis with their solvent-extractable counterparts for a suite of Krimmeridge clays. Organic Geochemistry 29, 1478–1505.

Peters, K.E., Moldowan, J.M., 1993. The Biomarker Guide: Interpreting Molecular Fossils in Petroleum and Ancient Sediments. Prentice Hall, Englewood Cliffs, NJ.

Peters, K.E., Walters, C.C., Moldowan, J.M., 2005. The Biomarker Guide, Biomarkers and Isotopes in Petroleum Exploration and Earth History. Cambridge University Press, New York.

Qiu, Y., Xu, L., Zhou, L., 1994. The hydrocarbon migration, accumulation and conservation: the reservoir bitumens of marine facies in South China for example. In: Qian, Z. (Ed.), New Technology for Experiment of Petroleum Geology. Geological Publishing House, Beijing.

Roberts, M.J., Snape, C.E., Mitchell, S.C., 1995. Hydropyrolysis: fundamentals, two-stage processing and PDU operation. In: Snape, C.E. (Ed.), Composition, Geochemistry and Conversion of Oil Shales. Kluwer, Dordrecht, pp. 277–294.

Rocha, J.D., Brown, S.D., Love, G.D., Snape, G.E., 1997. Hydropyrolysis: a versatile technique for solid fuel liquefaction, sulphur speciation and biomarker release. Journal of Analytical and Applied Pyrolysis 40–41, 91–103.

Rubinstein, I., Spyckerelle, C., Strausz, O.P., 1979. Pyrolysis of asphaltenes: a source of geochemical information. Geochimica et Cosmochimica Acta 43, 1–6.

Russell, C.A., Snape, C.E., Meredith, W., Love, G.D., Clarke, E., Moffatt, B., 2004. The potential of bound biomarker profiles released via catalytic hydropyrolysis to reconstruct basin charging history for oils. Organic Geochemistry 35, 1441–1459.

Sonibare, O.O., Snape, C.E., Meredith, W., Uguna, C.N., Love, G.D., 2009. Geochemical characterisation of heavily biodegraded tar sand bitumens by catalytic hydropyrolysis. Journal of Analytical and Applied Pyrolysis 86, 135–140.

Sun, Y., Meredith, W., Snape, C.E., Chai, P., 2008. Study on the application of hydropyrolysis technique to the description of organic matter in highly mature source rocks. Oil & Gas Geology 29, 276–282 (in Chinese with English abstract).

Tenger, Qin, J., Zheng, L., 2008. Hydrocarbon potential on excellent hydrocarbon source rock in Southern Guizhou Depression and its spatial–temporal distribution. Acta Geologica Sinica 82, 366–372 (in Chinese with English abstract).

Tian, H., Guo, T., Hu, D., Tang, L., Wo, Y., Song, L., Yang, Z., 2006. Marine lower assemblage and exploration prospect of Central Guizhou Uplift and its adjacent areas. Journal of Palaeogeography 8, 509–518 (in Chinese with English abstract).

Wang, S., Zheng, B., Cai, L., 1997. Oil and gas assessment and fossil pools in southern China. Marine Origin Petroleum Geology 2, 44–50 (in Chinese with English abstract).

Wu, W., 1989. The formation and destruction of palaeo-oil-reservoirs in the east of Guizhou province. Geology of Guizhou 18, 9–22 (in Chinese with English abstract).

Wu, L., Liao, Y., Fang, Y., Geng, A., 2012. The study on the source of the oil seeps and bitumens in the Tianjingshan structure of the northern Longmen Mountain structure of Sichuan Basin, China. Marine and Petroleum Geology 37, 147–161.

Wu, L., Liao, Y., Fang, Y., Geng, A., 2013. The comparison of biomarkers released by hydropyrolysis and by Soxhlet extraction from source rocks of different maturities. Chinese Science Bulletin 58, 373–383.

Xiang, C., Tang, L., Li, R., Pang, X., 2008. The episodic fluid flow of superimposed basin: evidence from fluid inclusion research in the Majiang area. Science in China (Series D) 38, s70–s77 (in Chinese with English abstract).

Xiao, X., 1992. Application of Organic Petrology in Petroleum and Gas Source Rock Evaluation. Guangdong Science and Technology Press, Guangzhou, China, pp. 68–69.

Xu, Z., Yao, G., Guo, Q., Chen, Z., Dong, Y., Wang, P., Ma, L., 2010. Genetic interpretation about geotectonics and structural transfiguration of the southern Guizhou depression. Geotectonica et Metallogenia 34, 20–31 (in Chinese with English abstract).

Xue, X., Zhao, Z., Zhao, P., 2007. Study on fossil oil pools and residual oil and gas pools in lower assemblage in Central Guizhou Uplift and its adjacent areas. Southern China Oil & Gas 20, 6–11 (in Chinese).

Zhang, Q., Tenger, Zhang, Z., Qin, J., 2007. Oil source of oil seepage and solid bitumen in the Kaili–Majiang Area. Acta Geologica Sinica 81, 1118–1124 (in Chinese with English abstract).

Zhao, Z., Zhu, Y., Xu, Y., 2004. Formation rules and prediction of exploration targets of Paleozoic–Mesozoic oil–gas reservoirs in Southern China. Acta Geologica Sinica 78, 710–720 (in Chinese with English abstract).

Zhou, J., Li, S., Yue, C., Zhong, N., 2006. Release and analysis of the biomarkers combined by covalent bound from higher evolved organic sediment. Acta Petrolei Sinica (Petroleum Processing Section) 22, 9–22 (in Chinese with English abstract).

Zhou, J., Li, S., Yue, C., Zhong, N., 2007. Study on hydropyrolysis of sedimentary organic matter and geochemical information of hydropyrolysates. Journal of Fuel Chemistry and Technology 35, 648–654.